SINGLE IMAGE ATMOSPHERIC VEIL REMOVAL USING NEW PRIORS

Alexandra Duminil *Jean-Philippe Tarel* *Roland Brémond*

COSYS-PICS-L
Univ. Gustave Eiffel
F-77454 Marne-la-Vallée, France
Email: alexandra.duminil@univ-eiffel.fr

ABSTRACT

From an analysis of the priors used in previous algorithms for single image defogging, a new prior is proposed to obtain a better atmospheric veil removal. The Naka-Rushton function is used to modulate the atmospheric veil according to empirical observations on synthetic foggy images. The parameters of this function are set from features of the input image. The algorithm is able to take into account different kinds of airborne particles and different illumination conditions. The proposed method is extended to nighttime and underwater images by computing the atmospheric veil on each color channel. Qualitative and quantitative evaluations show the benefit of the proposed algorithm.

***Index Terms*—** Visibility Restoration, Single Image Defogging, Bad Weather conditions, Atmospheric Veil, Naka-Rushton.

1. INTRODUCTION

Visibility restoration of outdoor images is a well-known problem in both computer vision applications and digital photography, particularly in degraded weather conditions such as fog, haze, rain and snow. These bad weather conditions cause visual disorders in the images such as loss of contrast and color shift, which contributes to reduce scene visibility. The lack of visibility can be particularly harmful for the performance of automated systems based on image segmentation [1], object detection [2], and thus needs visibility restoration as a pre-processing [3]. The decrease of contrast is due to the atmospheric veil for fog and haze. For rain and snow, it is due to far-away droplet occlusion.

This paper proposes two contributions: the first one is the use of a Naka-Rushton function in the inference of the atmospheric veil. The parameters of this function are estimated from the characteristics of the input image. The second contribution is the restoration of images with other kind of airborne particles and heterogeneous illumination, such as nighttime and underwater images, by processing each color channel separately.

The paper is organized as follows: Section 2 introduces the problem and related works. Section 3 presents the proposed visibility restoration method and section 4 shows experimental results with qualitative and quantitative evaluations and comparisons.

2. RELATED WORKS

2.1. Fog Visual Effect

Koschmieder's law is a simple optical model used to describe the visual effects of water airborne particles [3]. When fog and illumination are homogeneous along the ray going through x, the model is:

$$I(x) = J(x)t(x) + A(1 - t(x)) \tag{1}$$

where $I(x)$ is the foggy image, $J(x)$ the fog-free image, A the sky intensity and $x = (u, v)$ denotes the pixel coordinates in each image. The transmission $t(x) = e^{-kd(x)}$ describes the percentage of light which is not scattered, where k is the extinction coefficient which is related to fog density during daylight and $d(x)$ is the distance between the camera and the objects in the scene. The atmospheric veil is the last term in (1).

2.2. Daytime Image Defogging

Single image defogging algorithms can be divided into two categories. Image enhancement algorithms use ad-hoc techniques to improve the image contrast such as histogram equalisation and retinex, but scene depth is not taken into account. The second category we focus on, visibility restoration, are model-based and use Koschmieder's law. Due to the unknown depth, the problem is an ill-posed inverse problem that needs priors to be solved. Priors may be introduced as constrains or using a learning database.

In [3], geometric priors are introduced. He et al. [4, 5] introduced the Dark Channel Prior (DCP) as a method dedicated to color images. The idea is that an outdoor and fog-free image contains pixels of very low intensity on at least one of

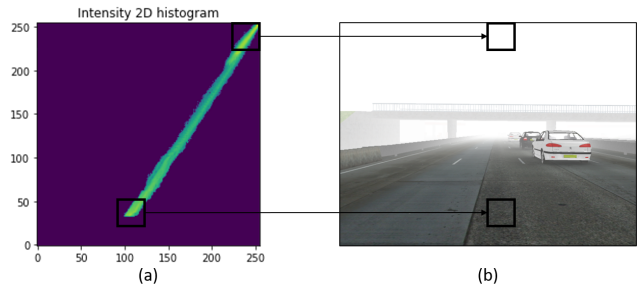

Fig. 1: Foggy pixels and veil pixel intensities: (a) histogram showing the link between pre-veil and veil pixel intensities (Mean of 50 images from the FRIDA database), (b) input foggy image.

the three color channels in any pixel neighborhood. Variants and extensions have been proposed such as [6, 7, 8].

In the last five years, learning-based methods have been proposed for defogging [9, 10, 11, 12, 13] usually based on CNN with supervised training. Fog is a quite rare phenomenon, so building a large and representative training database with pairs of images with and without fog is very difficult. This leads to generalization difficulties. More recently, GAN networks have been used [14], with partially supervised training databases but the learning control is complicated. Fog removal being a pre-processing, fast and computationally inexpensive algorithms are usually required. We thus focus here on algorithms with a very reduced number of parameters to be learned.

2.3. Hidden Priors in the DCP Method

In DCP [4, 5], a widely used parameter called ω was clearly introduced in the transmission map computation:

$$t(x) = 1 - \omega \min_c (\min_{y \in \Omega(x)} (\frac{I^c(y)}{A^c})) \quad (2)$$

were $\Omega(x)$ is the local patch centered on x, c the color channel, A the sky intensity, and I the image intensity. This parameter, usually set to $\omega = 0.95$, is constant across the entire image and was first introduced to mitigate over-restoration. According to [4], ω allows keeping a small amount of haze in front of distant objects, leading to more natural results.

This parameter can be seen as a prior which needs to be turned explicit and thus discussed. First, let us propose another interpretation of ω. The term $\min_c(\min_{y \in \Omega(x)}(I^c(y)))$ in the transmission equation (2) is a first estimation of the atmospheric veil, based on priors that the fog is white and locally smooth. But the obtained result is a mixture of the actual atmospheric veil and of the luminance of the seen objects. Let us name it the "pre-veil". The percentage of the pre-veil which corresponds to the real atmospheric veil is unknown,

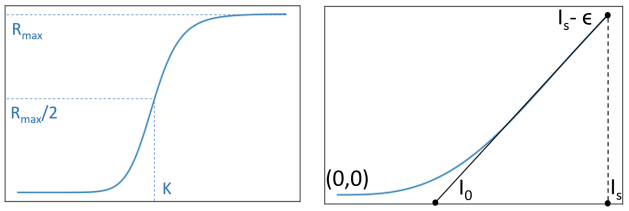

Fig. 2: Left: Naka-Rushton function with parameters R_{max}, K and n. Right: modulation function, with the shape of the left side of Naka-Rushton function, showing parameters I_s, I_0 and ϵ.

it is assumed to be constant across the image with value ω. Therefore, ω can be explicitly seen as a prior parameter: it is the assumed constant percentage of atmospheric veil in the pre-veil map.

The use of ω being seen as a prior on the atmospheric veil, we will test the validity of this prior in the next section.

3. SINGLE IMAGE ATMOSPHERIC VEIL REMOVAL

3.1. Is the use of ω a valid prior?

The usual way to compute the atmospheric veil from the pre-veil is to apply the parameter ω. To test the validity of this prior, we have to look at the link between the intensities in the true veil and in the pre-veil images. This can be performed only on a synthetic image database, and to achieve this we used the generator of the FRIDA database [7]. In this synthetic image database, the veil is computed using Koschmieder's law from the scene depth map. Thus, the atmospheric veil map can be computed for each generated foggy image. Fig. 1 (a) shows obtained histogram on fifty foggy images, with on the horizontal axis the pre-veil image intensities and on the vertical axis the intensities of the ground truth atmospheric veil.

Fig. 1(a) shows that the link between foggy pixel and associated veil intensities is roughly affine. The atmospheric veil has a high intensity in the sky region and a low intensity in the ground region near the camera. If this link is affine, it can not be modeled well with a single parameter such as ω. A function would be more relevant.

3.2. Modulation function as a prior

To avoid over-restoration at the bottom of the image while ensuring that the restoration is maximum at the top of the image, a modulation function f is necessary to compute the atmospheric veil from the pre-veil. The function should be smooth to avoid visual artefacts in the restored image.

From Fig. 1(a), for a good modulation of the pre-veil, the following constraints are proposed to chose an appropriate function f:

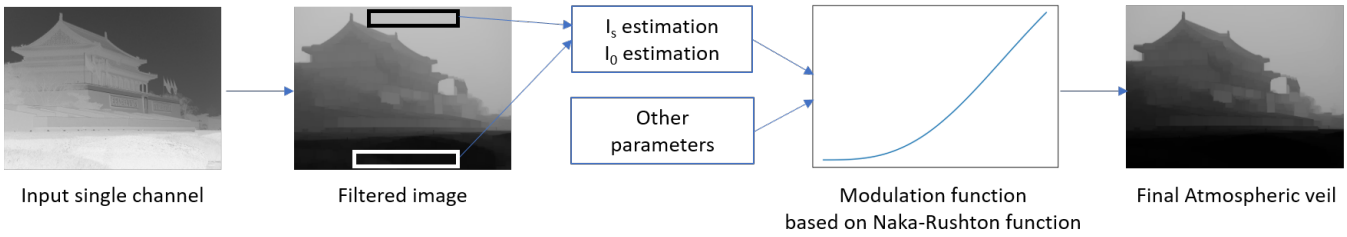

Fig. 3: Atmospheric veil estimation from the pre-veil using Naka-Rushton as a modulation function.

- The function f should be roughly linear on a large range of intensities. This range is denoted $[I_0, I_s]$. We introduce here the slope a of f at I_s, i.e $f'(I_s) = a$.
- The function is close to zero on the intensity range $[0, I_0]$, i.e for intensities near the camera where fog cannot be seen.
- The function and the restored image must not be lower than zero.
- I_s is the intensity of the clearest (sky) region. To avoid too dark values in the corresponding areas, $f(I_s)$ should be a little lower than I_s. We thus introduce a parameter ϵ such that $f(I_s) = I_s - \epsilon$.

Among the different functions we tested, the Naka-Rushton [15] function was the easier to tune. This function was first introduced to describe the biological response of a neuron, and was further used in computer graphics for the tone-mapping problem. It is defined as:

$$R(x) = R_{max}\frac{x^n}{x^n + K^n} \tag{3}$$

where R_{max} is its upper-bound, K is the horizontal position of the inflection point and n is related to the slope at the inflection point (see Fig. 2). The shape of the first part of the curve in Fig. 2 (left) fits our needs, as shown Fig. 2 (right). The inflexion point with coordinates $(K, R_{max}/2)$ should correspond to the modulation function f at I_s.

3.3. Naka-Rushton function parameters

R_{max}, K and n are the parameters of the Naka-Rushton function, while the parameters of the modulation function f are I_0, I_s, and ϵ. In the previous section, K was set to I_s. Following the previously explained constraints, $f(I_s)$ is set to $I_s - \epsilon$. Thus, $R_{max} = 2(I_s - \epsilon)$. The slope at I_s is set to a. This slope in the Naka-Rushton function being $nR_{max}/4K$, we have $n = \frac{2I_s a}{I_s - \epsilon}$. It follows that $a = \frac{I_s}{I_s - I_0}$. Finally, the proposed modulation function f is:

$$f(x) = f_0\frac{x^n}{x^n + k^n} \tag{4}$$

where $f_0 = 2(I_s - \epsilon)$, $k = I_s$, $n = \frac{2I_s a}{I_s - \epsilon}$ and $a = \frac{I_s}{I_s - I_0}$.This modulation function has only three parameters: I_0, I_s, and ϵ. The last one needs to be chosen as a small value, the other two can be computed from the input image.

In Fig. 1(b), I_s is the intensity of the sky and I_0 is the intensity of the ground close to the camera. We have investigated how I_0 and I_s can be best estimated. Taking the maximum of the image intensities for I_s and the minimum for I_0 is too sensitive to noise. Therefore, I_0 and I_s are computed by taking, respectively, the minimum and the maximum of the input foggy image after applying, respectively, morphological closing and opening filters. The veil processing is shown in Fig. 3.

3.4. Beyond the White Fog Prior

In order to better handle colored atmospheric veil, we propose a simple method: processing each color channel separately with our algorithm. This is possible only because the proposed atmospheric veil removal method is able to process gray-level images thanks to the use of the modulation function prior. By processing each color channel separately, I_s is estimated on each channel and thus the color of the veil is inferred.

4. EXPERIMENTAL RESULTS

The proposed algorithm is compared with six state-of-the-art algorithms included three prior-based methods and three learning-based methods: DCP [5], NBPC [6], Zhu et al [8], AOD Net [12], Dehaze Net [9] and GCA Net [13]. We selected algorithms with public codes. For each algorithm, all input parameters have been optimized. But the ω parameter in DCP is fixed to 0.95. For each parameter, several values have been tested on four databases using SSIM and PSNR as criterions. Firstly, a quantitative comparison with synthetic images from the public FRIDA database [7], the RESIDE SOTS outdoor dataset [16], NTIRE20 dataset and O-HAZE dataset [17] is carried out. Secondly, a qualitative comparison is shown on real world images.

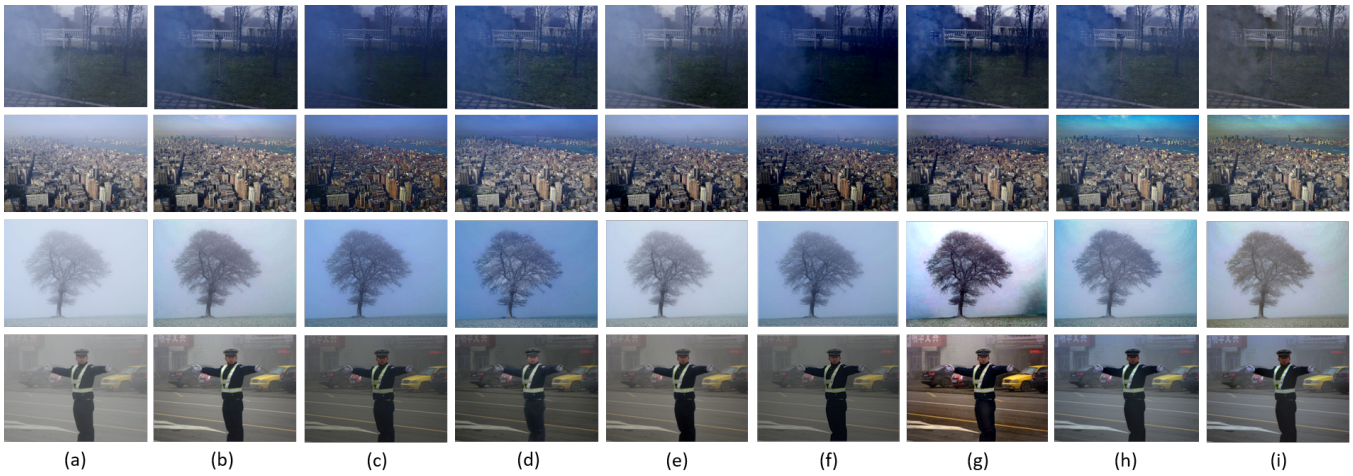

Fig. 4: Comparison of fog removal results on real world image (see additional examples in the supplementary material): (a) input foggy images, (b) DCP, (c) NBPC, (d) Zhu et al., (e) Dehaze Net, (f) AOD Net (g) GCA Net, (h) Ours W and (i) Ours C.

SSIM/PSNR	FRIDA	SOTS	NTIRE20	O-HAZE
DCP	0.70/12.26	0.89/18.91	0.44/12.77	**0.66**/16.95
NBPC	0.75/11.59	0.89/18.07	0.41/12.24	0.61/15.85
Zhu et al.	0.72/12.15	0.88/16.06	0.45/11.98	**0.66**/16.58
AODNet	0.73/10.73	0.85/19.39	0.41/11.98	0.54/15.04
DehazeNet	0.65/10.87	**0.90/23.41**	0.44/12.33	0.60/15.41
GCANet	0.70/**12.79**	**0.91/22.68**	0.47/12.82	0.61/16.43
Ours W	**0.81/12.62**	0.85/17.23	**0.51/13.16**	0.65/17.02
Ours C	**0.81/12.27**	0.82/16.77	**0.51/13.90**	**0.67/18.32**

Table 1: Comparison in term of SSIM and PSNR on four different datasets: 50 images of FRIDA, SOTS datasets, 45 images of NTIRE20 and O-HAZE datasets. Ours W correspond to our main algorithm assuming white fog and Ours C correspond to the color variant of Sec. 3.4.

4.1. Quantitative Evaluation

Results are shown in Tab. 1 and illustrate that all methods are competitive but the proposed method outperforms the others with both criterions on FRIDA, SOTS and O-HAZE datasets. However, the results on SOTS dataset show that the proposed algorithm is less efficient than other on images where the veil is spatially close to uniform.

4.2. Qualitative Evaluation

Real world images from previous works on fog removal have been used for a qualitative comparison. On Fig. 4, DCP, NBPC and Zhu et al. algorithms remove the fog with good results. However, DCP images are bright and contrasted, while NBPC and Zhu et al.'s results are darker and more faded. The learning-based method AOD Net provides faded and dark results but with a reduced number of halos. It appears in the tree and buildings images that Dehaze Net method retains far away haze. It better works on images with colored sky regions by avoiding artefacts and blue-shift distortions unlike most of other algorithms. GCA Net produces artefacts in sky region of the tree image but provides good and colored results in others particularly in the last line image.

The first version of our algorithm (Our W) provides bright results and remove the haze over the entire images. The second version (Our C) allow to reduce color distortions by applying the function on each RGB channels.

5. CONCLUSION

We have reinterpreted the DCP method in term of three priors. We propose to improve the third prior, associated to ω, with a smooth modulation function as a prior to estimate the atmospheric veil from the pre-veil. The input parameters of this function are automatically estimated according to the input image pixel intensities in light (sky) and dark (ground) regions. The proposed method provides good results on both synthetic and real world images from objects at any distances.

To extend the proposed algorithm to rain, smoke, dust and other colored airborne particles, we process each color channel separately, in order to remove colored components on every color channels. This allows to apply the algorithm to nighttime images as well as underwater images. The proposed algorithm should be carefully evaluated on these diverse conditions. This is not easy with real world images, as ground truth are very difficult to build.

A few color artifacts have been observed when restoring sky regions of objects at large distances. In the future, we will thus investigate the limits of the proposed algorithm, trying to avoid artifacts and preserve a better color consistency.

6. REFERENCES

[1] Maxime Tremblay, Shirsendu Halder, Raoul De Charette, and Jean-François Lalonde, "Rain rendering for evaluating and improving robustness to bad weather," vol. accepted, 2020.

[2] Jiajun Lu, Hussein Sibai, Evan Fabry, and David Forsyth, "NO Need to Worry about Adversarial Examples in Object Detection in Autonomous Vehicles," *arXiv:1707.03501 [cs]*, July 2017.

[3] Nicolas Hautière, Jean-Philippe Tarel, and Didier Aubert, "Towards fog-free in-vehicle vision systems through contrast restoration," in *IEEE Conference on Computer Vision and Pattern Recognition (CVPR'07)*, Minneapolis, Minnesota, USA, 2007, pp. 1–8, http://perso.lcpc.fr/tarel.jean-philippe/publis/cvpr07.html.

[4] Kaiming He, Jian Sun, and Xiaoou Tang, "Single image haze removal using dark channel prior," in *2009 IEEE Conference on Computer Vision and Pattern Recognition*. IEEE, 2009, pp. 1956–1963.

[5] Kaiming He, Jian Sun, and Xiaoou Tang, "Single Image Haze Removal Using Dark Channel Prior," *IEEE Transactions on Pattern Analysis and Machine Intelligence*, vol. 33, no. 12, pp. 2341–2353, Dec. 2011.

[6] Jean-Philippe Tarel and Nicolas Hautiere, "Fast visibility restoration from a single color or gray level image," in *2009 IEEE 12th International Conference on Computer Vision*, Kyoto, Sept. 2009, pp. 2201–2208, IEEE.

[7] J-P Tarel, N. Hautiere, L. Caraffa, A. Cord, H. Halmaoui, and D. Gruyer, "Vision Enhancement in Homogeneous and Heterogeneous Fog," *IEEE Intelligent Transportation Systems Magazine*, vol. 4, no. 2, pp. 6–20, 2012.

[8] Mingzhu Zhu, Bingwei He, and Qiang Wu, "Single Image Dehazing Based on Dark Channel Prior and Energy Minimization," *IEEE Signal Processing Letters*, vol. 25, no. 2, pp. 174–178, Feb. 2018.

[9] Bolun Cai, Xiangmin Xu, Kui Jia, Chunmei Qing, and Dacheng Tao, "DehazeNet: An End-to-End System for Single Image Haze Removal," *IEEE Transactions on Image Processing*, vol. 25, no. 11, pp. 5187–5198, Nov. 2016.

[10] Wenqi Ren, Si Liu, Hua Zhang, Jinshan Pan, Xiaochun Cao, and Ming-Hsuan Yang, "Single Image Dehazing via Multi-scale Convolutional Neural Networks," in *Computer Vision – ECCV 2016*, Bastian Leibe, Jiri Matas, Nicu Sebe, and Max Welling, Eds., Cham, 2016, Lecture Notes in Computer Science, pp. 154–169, Springer International Publishing.

[11] Tim Meinhardt, Michael Moeller, Caner Hazirbas, and Daniel Cremers, "Learning Proximal Operators: Using Denoising Networks for Regularizing Inverse Imaging Problems," in *2017 IEEE International Conference on Computer Vision (ICCV)*, Venice, Oct. 2017, pp. 1799–1808, IEEE.

[12] Boyi Li, Xiulian Peng, Zhangyang Wang, Jizheng Xu, and Dan Feng, "An All-in-One Network for Dehazing and Beyond," *arXiv:1707.06543 [cs]*, July 2017.

[13] D. Chen, M. He, Q. Fan, J. Liao, L. Zhang, D. Hou, L. Yuan, and G. Hua, "Gated Context Aggregation Network for Image Dehazing and Deraining," in *2019 IEEE Winter Conference on Applications of Computer Vision (WACV)*, Jan. 2019, pp. 1375–1383, ISSN: 1550-5790.

[14] Deniz Engin, Anil Genc, and Hazim Kemal Ekenel, "Cycle-Dehaze: Enhanced CycleGAN for Single Image Dehazing," in *2018 IEEE/CVF Conference on Computer Vision and Pattern Recognition Workshops (CVPRW)*, Salt Lake City, UT, USA, June 2018, pp. 938–9388, IEEE.

[15] K. I. Naka and W. a. H. Rushton, "S-potentials from colour units in the retina of fish (Cyprinidae)," *The Journal of Physiology*, vol. 185, no. 3, 1966.

[16] B. Li, W. Ren, D. Fu, D. Tao, D. Feng, W. Zeng, and Z. Wang, "Benchmarking Single-Image Dehazing and Beyond," *IEEE Transactions on Image Processing*, vol. 28, no. 1, pp. 492–505, Jan. 2019, Conference Name: IEEE Transactions on Image Processing.

[17] Codruta O. Ancuti, Cosmin Ancuti, Radu Timofte, and Christophe De Vleeschouwer, "O-HAZE: A Dehazing Benchmark With Real Hazy and Haze-Free Outdoor Images," 2018, pp. 754–762.